Proceedings of the 2011 International Conference on Machine Learning and Cybernetics, Guilin, 10-13 July, 2011

REAL-TIME CAMERA ANOMALY DETECTION FOR REAL-WORLD VIDEO SURVEILLANCE

YUAN-KAI WANG[1], CHING-TANG FAN[2], KE-YU CHENG[1], PETER SHAOHUA DENG[3]

[1]Department of Electrical Engineering, Fu Jen University, New Taipei, Taiwan
[2]Graduate Institute of Applied Science and Engineering, Fu Jen University, New Taipei, Taiwan
[3]Department of Information Management, Central Police University, Taoyuan, Taiwan
E-MAIL: [1]ykwang@ieee.org, [2]bevis@islab.tw

Abstract:

This paper proposes an automatic event detection technique for camera anomaly by image analysis, in order to confirm good image quality and correct field of view of surveillance videos. The technique first extracts reduced-reference features from multiple regions in the surveillance image, and then detects anomaly events by analyzing variation of features when image quality decreases and field of view changes. Event detection is achieved by statistically calculating accumulated variations along temporal domain. False alarms occurred due to noise are further reduced by an online Kalman filter that can recursively smooth the features. Experiments are conducted on a set of recorded videos simulating various challenging situations. Compared with an existing method, experimental results demonstrate that our method has high precision and low false alarm rate with low time complexity.

Keywords:

Video surveillance; camera anomaly; camera tampering; camera sabotage; online Kalman filtering

1. Introduction

Image quality is crucial to video surveillance with respect to both automated detection and human perception. Clear images of good contrast, satisfactory sharpness and sufficient illumination are necessary for event detection and identification and recognition of objects appeared in a monitored environment. In addition, correct field of view(FOV) is also significant for video surveillance. Incorrect FOV induced by intentional or accidental camera movement is abnormal for the monitoring of a specific site and a camera anomaly alert shall be issued. An automatic anomaly detection method is necessary for a large visual surveillance system installed with a huge amount of cameras. The benefits of the anomaly detection method are that the system can continuously diagnose camera's status without tremendous human labors but in the danger of carelessness, and real-time anomaly alerts can prompt actions and prevent from crimes.

However, the anomaly detection is not a trivial task when considering complex surveillance situations happened in real world. Intentional sabotage to camera, such as spray painting, blockage, defocusing, and redirecting**[1-4]**, has to be detected, of course. Accidental tampering by careless maintenance, dusting fierce wind, and earthquake, which produces permanent anomaly in either degradation of image quality or abnormal FOV, is also true event. But many false alarms challenge the anomaly detection. These false alarms can be easily produced by a lot of unintentional factors from humans and natural phenomena in environment.

For example, wrong detection of blockage happens when a crowd moves or a large object passes in front of the camera. Transient shakes by slight earthquake and wind may not permanently change the FOV of cameras, but can easily raise the rate of false alarms. Illumination problems induced by light change and weather can both degrade image quality and change all pixel values, which will lead to any kind of erroneous anomaly event. Low false-alarm rate with respect to those situations is therefore very challenging.

In this paper, we propose a camera anomaly detection method tolerant against most of the unsettled cases which induce false alarms. For real-time detection of camera anomalies, a reduced-reference method is devised. Image features are extracted to be the reference of normality of image quality and FOV. Significant change of image features sustained for a period of time is recognized as an anomaly event. For most anomaly events, we extract the features from full image. But a region mechanism is applied for the redirecting event. The region is defined as the rigid region where has lower movement in the full image, and then the features are extracted only inside region.

But mercurial conditions in the real-world cause a lot of

978-1-4577-0308-9/11/$26.00 ©2011 IEEE

noise and produce high false-alarm rate. An online Kalman filter can recursively smooth the sequential feature and improve the real-time decision.

The reminder of this paper is organized as follows. In Section 2, a review of related works is given. Section 3 describes the reduced-reference features for camera anomaly detection. Section 4 deals with the online Kalman filtering to improve the robustness of camera anomaly detection for real-world situations, and our camera anomaly decision approach is presented in Section 5. Experimental results are provided in Section 6 and conclusions and discussions are followed in Section 7.

2. Related Works

The reference image used in camera anomaly detection is often the first image defined by human. However, in image quality assessment**[5,6]**, there are three approaches to draw inferences of image quality about the target image. These are full-reference(FR), no-reference(NR) and reduce-reference (RR). The difference among the three approaches is the dimension of the reference data. FR metrics are proposed based on a reference image whose size is equivalent to the target image and a pixel-based comparison between the reference and target images is used. On the contrary, NR metric which uses only current frame does not need reference data ahead with the sacrifice of accuracy. Not so extreme, the reference data which is less than the size of input image even as little as only one value is called RR metric.

Most of the previous camera tampering detection methods belong to the FR approach, because they adopt statistically-modeled background image as reference frames to eliminate variations from noises and cluttered scenes. In **[1]**, the entropy, edges and the zero-mean normalized cross correlation were computed from the background image modeled by nonparametric kernel density method, and the rate of change will govern the decision results of image occlusion, image defocus and change of FOV, respectively. Aksay et al.**[2]** employed wavelet domain methods in background image obtained by mixture of Gaussians to detect the sabotages such as deliberately obscuring the camera view, covering the lens with a foreign object, and spraying or defocusing the camera lens. Saglam and Temizel**[3]** also compared the newest frame with an adaptively-updated background image. They kept track of the moving areas of the camera's view and employed a region-based feature extraction to detect camera tampering. These methods depend on the success of background modeling. But the background modeling is still not robust too the real-world challenges such as large/crowd movement and illumination problems. Therefore these methods are prone to fail in these situations. On the other hand, these background-modeling methods rely on pixel-based computation and computational loading.

NR metric which does not have the computational overhead problem is vis-à-vis FR metric. There was an application using NR metrics to classify blurred images in **[7]**. They compared Canny edge components with Sobel edge components in current frame. When the number of Canny edge components is larger, the image is classified to be a blurred one, and vice versa. But the experiments showed that it can misclassify when many faces appear in the image.

The RR metric is a good compromise between the FR and NR methods. Ribnick et al.**[4]** extracted color histogram and gradient information from previous frames. The camera tampering can be decided from a set of conditions which is based on the mean, variance, skewness, and kurtosis of those features. However, in RR metric, features as reduced reference information to represent the scene have to be carefully designed in order to endure challenging conditions.

3. Reduced-Reference Features

A good feature of camera anomaly detection has advantage of low sensitive to influence by noises and high sensitive to concern about true alarm, but there is no such a feature that can take these two conditions into account.

The pixel-based edge energy E_t at frame t can be regarded as the aggregate number of edge pixels in an image. The Canny edge detection which includes noise reduction is traced edges through the image and hysteresis thresholding. The sum of Canny detector's edges divided by the dimension of an image is used for normalized E_t into [0,1]. The equation for E_t can written as follows:

$$E_t = \frac{1}{N}\sum^{N} I_t^E(x,y), where\ I_t^E(x,y) = \begin{cases} 1, & if\ (x,y)\ is\ edge \\ 0, & otherwise \end{cases} \quad (1)$$

where N is the total pixel numbers and $I_t^E(x,y)$ is the Canny edge Image at frame t.

Region-based edge energy has less reference pixels and more sensitive than image-based edge energy. We offer each region SR^j for a region-based edge energy E_t^j at frame t. Therefore, a region-based edge energy's set $\vec{E}_t$ is collected by E_t^j, as shown below.

$$\vec{E}_t = \{E_t^j | 1 \le j \le J\} \quad (2)$$

$$E_t^j = \sum_{(x,y)\in SR^j} I_t^E(x,y) \quad (3)$$

The standard deviation of graylevel's image plane could be indicated the complexity of a scene. The property of

standard deviation which has less affected by the change of illumination is more meaningful and stable than graylevel's mean $\bar{g}_t$ at frame t in an image. The image-based graylevel standard deviation energy which is calculated by $\bar{g}_t$ is given by

$$\Sigma_t = \sqrt{\frac{1}{N}\sum(I_t(x,y) - \bar{g}_t)^2}, \quad (4)$$

where $\bar{g}_t = \frac{1}{N}\sum I_t(x,y)$.

If there are non-uniform light source which will produce too bright areas in the scene, Σ_t will increase easily. The graylevel standard deviation energy Σ_t^l in block $l = \{1,2,\ldots\ldots,L\}$ could resist this problem. We divide the image into L blocks that each block's size is $u*u$ and overlapped $u/2$. The Σ_t^l is defined as

$$\Sigma_t^l = \sqrt{\frac{1}{u^2}\sum_{(x,y)\in B_l}(I_t(x,y) - \bar{g}_t^l)^2}, \quad (5)$$

where the graylevel's mean of block B_l is $\bar{g}_t^l = \frac{1}{u^2}\sum_{(x,y)\in B_l} I_t(x,y)$. Given that block-based graylevel standard deviation energy $\bar{\Sigma}_t^L$ which is the mean of L blocks, we obtain

$$\bar{\Sigma}_t^L = \frac{1}{L}\sum_{l=1}^{L}\Sigma_t^l. \quad (6)$$

4. Online Kalman Filterng

In this section, we utilize the online Kalman filtering(OKF) which is applied the Kalman filter on temporal domain into the proposed general anomaly detection to the problem of real-world applications including noises.

For each feature's energy f_t at frame t, it can be grouped its first derivative f_t' together as a vector $\boldsymbol{f}_t$. A simple online dynamic system addresses the temporal problem of trying to smooth the state of a continuous-time controlled process that is governed by the linear stochastic difference equation

$$\boldsymbol{f}_t = \mathbf{F}\boldsymbol{f}_t + \boldsymbol{w}_t, \ \boldsymbol{f}_t = \begin{bmatrix} f_t \\ f_t' \end{bmatrix}, \quad (7)$$

where the random variable $\boldsymbol{w}_t \sim N(0, \mathbf{Q})$, which is an i.i.d. standard normals with covariance $\mathbf{Q}$, represents the process noise and the matrix $\mathbf{F}$ signifies state transition model. The measurement vector $\boldsymbol{z}_t$, gathered measurement z_t and its first derivative z_t' together, of the true state $\boldsymbol{f}_t$ is made according to

$$\boldsymbol{z}_t = \mathbf{H}\boldsymbol{f}_t + \boldsymbol{v}_t, \ \boldsymbol{z}_t = \begin{bmatrix} z_t \\ z_t' \end{bmatrix}, \quad (8)$$

where $\boldsymbol{v}_t \sim N(0, \mathbf{R})$ is also a zero mean multivariate normal distribution with covariance $\mathbf{R}$, and $\mathbf{H}$ is the measurement model which maps the true state space into the measured space.

The OKF is a recursive method based on online linear dynamic system. The current state is only computed by the smoothed state from the previous time step and the current measurement. There is no extra history of measurements and states needed. The priori state $\hat{\boldsymbol{f}}_{t|t-1}$ at time t could smooth by the previous posteriori state $\hat{\boldsymbol{f}}_{t-1|t-1}$ through matrix $\mathbf{F}$, as shown below. $\hat{\boldsymbol{f}}_{t|t-1} = \mathbf{F}\hat{\boldsymbol{f}}_{t-1|t-1}$. We suppose the feature energies of the surveillance's images between the two of two continuous frames would not undergo considerable fluctuation, that is $f_t = f_{t-1} + f_{t-1}'$ and $f_{t-1}' = f_t'$, so transition matrix $\mathbf{F}$ becomes $\mathbf{F} = \begin{bmatrix} 1 & 1 \\ 0 & 1 \end{bmatrix}$.

Another variable which has to smooth is the priori error covariance matrix $\mathbf{P}_{t|t-1}$, that is a measure of the estimated accuracy of the priori state. Through transition matrix $\mathbf{F}$ and noises' covariance $\mathbf{Q}$, the relationship between $\mathbf{P}_{t|t-1}$ the previous error covariance $\mathbf{P}_{t-1|t-1}$ is as follows:

$$\mathbf{P}_{t|t-1} = \mathbf{F}\mathbf{P}_{t-1|t-1}\mathbf{F}^{\mathrm{T}} + \mathbf{Q}, \ \mathbf{P}_0 = \begin{bmatrix} 1 & 0 \\ 0 & 1 \end{bmatrix}. \quad (9)$$

After the smoothed step, the current priori results have to blend with current measurement information to refine the state estimate to current posteriori state $\hat{\boldsymbol{f}}_{t|t}$ and current posteriori covariance $\mathbf{P}_{t|t}$. $\hat{\boldsymbol{f}}_{t|t}$ and $\mathbf{P}_{t|t}$ are given by

$$\hat{\boldsymbol{f}}_{t|t} = \hat{\boldsymbol{f}}_{t|t-1} + \mathbf{K}_t\tilde{\boldsymbol{d}}_t, \quad (10)$$

$$\mathbf{P}_{t|t} = (\mathbf{I} - \mathbf{K}_t\mathbf{H})\mathbf{P}_{t|t-1}, \quad (11)$$

where the measurement residual error $\tilde{\boldsymbol{d}}_t$ and the optimal Kalman gain $\mathbf{K}_t$ can be expressed as

$$\tilde{\boldsymbol{d}}_t = \boldsymbol{z}_t - \mathbf{H}\hat{\boldsymbol{f}}_{t|t-1}, \quad (12)$$

$$\mathbf{K}_t = \mathbf{P}_{t|t-1}\mathbf{H}^{\mathrm{T}}(\mathbf{H}\mathbf{P}_{t|t-1}\mathbf{H}^{\mathrm{T}} + \mathbf{R})^{-1}. \quad (13)$$

The measurement residual error $\tilde{\boldsymbol{d}}_t$ is the distance between the smoothed state and measurement. The measurement is almost regard to the true state, that is $g_t \approx f_t$ and $g_t' \approx f_t'$. The reason of their difference is come from the noises. The

measurement matrix **H** can be written as $\mathbf{H} = \begin{bmatrix} 1 & 0 \\ 0 & 1 \end{bmatrix}$. The optimal Kalman gain is controlling the weighting between state and measurement. When $\mathbf{K}_t$ is greater, the measurement is more paid attention. Besides, the smoothed state is more likely to be affected by the noises.

The noises' covariance **Q** and **R** would affect the smooth effects, when those two are more closer to zero, the results would more smooth, but the response time would be increased relatively. Figure 1 shows the comparison of having or not the OKF, a significant noise reduction in OKF implemented in temporal energy.

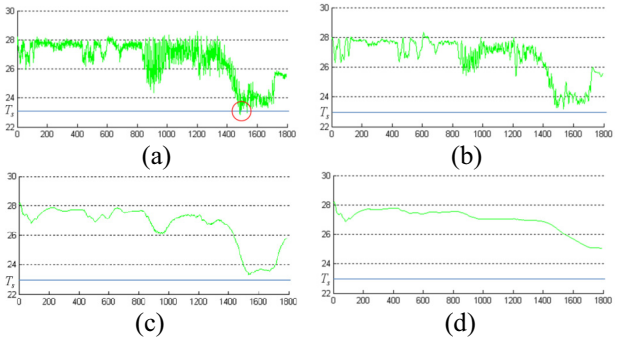

Figure 1. Comparison of filtering for an edge energy trend chart in temporal domain. (a) Result without OKF, there are two false alarms at the number of 1400 to 1600 frames. The result uses OKF, for all $\mathbf{R} = [e^{-1}, \ e^{-1}]^T$, (b) $\mathbf{Q} = [e^{-4}, \ e^{-4}]^T$, (c) $\mathbf{Q} = [e^{-8}, \ e^{-8}]^T$, and (d) $\mathbf{Q} = [e^{-16}, \ e^{-16}]^T$.

5. Camera Anomaly Decision

The degradation of each energy's trend in temporal domain could be mixed up and discovered a camera anomaly event. A simple and effective way to detect the event is using a threshold to divide each of energy into anomaly or not. The threshold of image-based edge energy E_t, image-based graylevel standard deviation energy Σ_t, and block-based graylevel standard deviation energy $\bar{\Sigma}_t^L$ is T_E, T_Σ, and $T_{\bar{\Sigma}}$ respectively. An adaptive threshold set which is corresponding to region-based edge energy is defined as

$$\mathbf{T}_E = \{T_E^j = \beta E_t^j | 1 \le j \le J\}, \ \text{where } 0 < \beta < 1. \quad (14)$$

For each region E_t^j, a threshold T_E^j is defined as a small ratio of E_t^j which is mined at time $\hat{t}$.

Through thresholding of energies at every subsequence, a sketchy camera state *St* is obtained by a sketchy camera anomaly decision(SCAD)

$$S_t = \begin{cases} 1, & if\ f(E_t < T_E) \wedge (\Sigma_t < T_\Sigma) \wedge (\bar{\Sigma}_t^L < T_{\bar{\Sigma}}) \\ 2, & else\ if\ (J_E > [J/2]) \\ 0, & otherwises, \end{cases} \quad (15)$$

where the number of region-based edge energies' thresholding result can be written as

$$J_E = \sum_{j=1}^{J} f(\bar{\Sigma}_t^j - T_E^j), \ f(x) = \begin{cases} 1, & if\ x < 0 \\ 0, & otherwises. \end{cases} \quad (16)$$

We defined three classes of the state of camera, where S_t=0 is meaning for normal state and others are the anomaly states which are needed to alarm. The anomaly states are subdivided into two cases: redirecting case and miscellaneous case, which are expressed as S_t=1 and S_t=2 respectively. The reason we separate redirecting cases expressly is that camera redirection is more critical than other anomaly cases. For other cases, human can instinctively found out the anomaly reason, but the redirected image would possible like the image before redirection.

Even the sketchy camera state is acquired; it still cannot be the anomaly decision result, because the sudden anomaly state has strong possibly caused by noises. We build a linear cumulative strategy upon the SCAD as follow

$$C_t = \begin{cases} \max(0, C_{t-1} - \gamma), & if\ S_t = 0 \\ \min(1, C_{t-1} + \lambda), & otherwises, \end{cases} \quad (17)$$

where the increased parameter γ and decreased parameter λ could be filtered out the misjudgment caused by noises, and both are ranged in [0,1]. The camera anomaly is decided by C_t which is alarmed at $C_t = 1$ and initial at zero. The parameters γ and λ are often very small. When γ is larger, C_t is more easily decreased to minimum, zero; when λ is larger, C_t is more easily increased to maximum, one.

The correct decision is depended on accurate feature's trend in temporal domain, but the features, influenced by noises, are not stable in the real world. The noises would be produced by real-world scenes and the cameras. The real-world noises which are bring from uncertain situations are called "process noises" and the camera noises which are resulted from cameras are called "measurement noises". The measurement noises are able to smooth by this general decision part, but the process noises which are violent and variable may not be dealed with. An online Kalman filtering method could be applied to reduce this problem.

6. Experimental Results

As there are no datasets available for camera anomaly

detection, we captured a certain amount of simulation scenarios to test the proposed methods and the newest camera tampering method**[3]**, which has also compare with previous methods and get the best results, in the literature. In particular, there have few simulation scenarios which are imitated for special cases without any camera anomaly to reflect real-world events. The testing videos captured from the analog camera are digitized by using VGA resolution, 30 frames per second, and encoding with MPEG1. All of the testing video has contain 1800 to 2700 frames and at least 30 seconds of normal surveillance scenarios before the anomaly events happened, that is taking some algorithms needed background modeling time into consideration. There are total 75 testing videos which are including 57 videos with anomaly events and 18 videos without any camera anomaly. An anomaly video has only one event inside.

The anomaly events contain four behaviors: camera self-defocusing, spray-paint, covering, and redirecting in our testing videos. The examples of anomaly sequences are shown in Figure 2. The camera self-defocusing is meaning the camera defocusing by its unsuitable focal length. We post a transparent film above the camera and take a colorful spray to painting on it as a spray-paint event. The covering events could come from diversified properties, where a cloth and a cardboard are the common tools. Sometimes bottles and picture would be taken to cover the view of cameras, but it is quite difficult to detect as an anomaly event. As shown in Figure 3, a picture which is similar to real-world and a bottle which does not block the whole frame are easy confusing the anomaly judgment. The case that a camera is turned to make it point to a different direction is called a redirecting event.

There are three special cases without any camera anomaly are simulated for typical surveillance scenarios such as large objects passing through the scene(Figure 4), water dropping on camera temporary, and camera vibration by earthquake.

In the experiments, the sensitivity setting is used as normal, that threshold as follows: $T_E = 0.02, T_\Sigma = 10, T_\Sigma = 4$, and the parameters are $\hat{t} = 200$, $k = 8, u = 8, \alpha = 0.1, \beta = 0.25$, $\gamma = 0.07, \lambda = 0.07$. The parameter σ_0 is initialized at 30. As a classification task, there are usually four given classification of an observation with the desired correct result, which are true positives, true negatives, false positives, and false negatives. There has only one classification result corresponding to one video in our experiments. The number of true positives, that the videos have correct alarm after the ground truth's event happened time, is called *TP*. The number of true negatives(*TN*) is composed from a non-anomaly video which have no detected result. A video, containing an anomaly event but not detected, is one of false negative number(*FN*). There are two cases for calculating the number

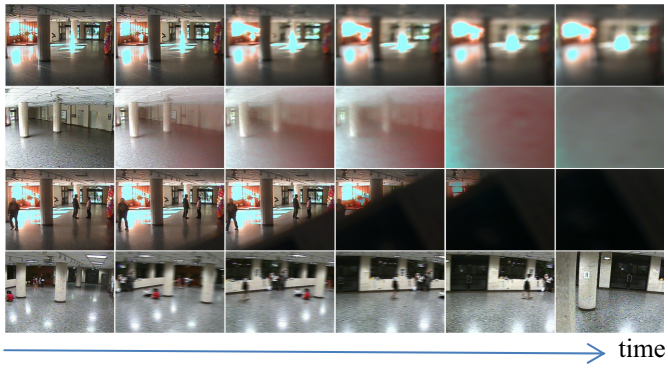

Figure 2. The example of anomaly events. The top row of images it the effect of camera self-defocusing. The second row is a spray-paint event, and the third row is a covering event. The bottom row is a camera redirecting event.

(a) (b)

Figure 3. Special covering events in real-world cases. (a) Coverd by a picture. (b) Coverd by a bottle.

Figure 4. A special case which has a large object passing through the scene without any camera anomaly.

of false positives(*FP*), that is a false alarm in a non-anomaly video or alarming before event happened in an anomaly-containing video.

The performance of the camera anomaly detection is measured in terms of precision rate R_p, recall rate R_r and false alarm rate R_{fa}, as shown below.

$$R_P = \frac{TP}{TP+FP} \times 100\% \quad (18)$$

$$R_R = \frac{TP}{TP+FN} \times 100\% \quad (19)$$

$$R_{FA} = \frac{FP}{TN+FP} \times 100\% \quad (20)$$

Data in Table 1. The Result Compares Accuracy Rate Precision Rate And Recall Rate Between Different Algorithms. The Ideal Case show that the precision of our proposed method is higher than other method, and OKF is significantly effective for enhancing the precision rate. When our make an alarm, it has 96.55% rate actually happen an anomaly event. There is one false negative in proposed method that is leading to give 98.25% recall rate which is lower than **[3]**. Unfortunately, **[3]** gives too high false alarm rate even it has higher recall rate. This is because our normal

cases which are all special cases without any camera anomaly and these cases could not avoid by **[3]**. Camera vibration is quite difficult avoided by background based methods in particular. Our proposed has respected to these really happened cases by multiple considering. The false alarm can be first avoided with the feature selection and linear cumulative strategy. While OKF is implemented, the false alarm rate is reduced effectively again.

TABLE 1. THE RESULT COMPARES ACCURACY RATE PRECISION RATE AND RECALL RATE BETWEEN DIFFERENT ALGORITHMS. THE IDEAL CASE IS TP=57, TN=22, FP=0, FN=0, R_R =100%, R_P=100% AND R_{FA}=0%.

Algorithms	*TP*	*TN*	*FP*	*FN*	R_P	R_R	R_{FA}
Ali Saglam et al.[3]	40	0	35	0	53.33%	100%	100%
Proposed method (without OKF)	56	11	7	1	88.89%	98.25%	38.88%
Proposed method	56	16	2	1	96.55%	98.25%	11.11%

The algorithms in the experiments were programed by C language based on OpenCV**[8]** without multi-thread, and they were performed on a 2.67GHz Intel Core i7 PC. Our algorithms can achieve rates of 20.8 FPS for one camera on both OKF implemented or not. It shows that our proposed with OKF does not have additional computation overhead. There have only 12.8 FPS for **[3]**. The advantage on reduced reference than full reference method is revealed apparently. While the amount of camera is always huge in the surveillance, our method could make cost down by relatively few hardware requirements.

7. Conclusions

In this work, the procedure of reduced reference and multi-filtering method for camera anomaly detection has been investigated. The multiple regions are automatic built by rigid parts selection, and features in the region are extracted to detect for image quality decreases and field of view changes. A new decision method based upon a linear cumulative strategy of two growth factors and an online Kalman filtering was derived. The computational complexity of the proposed algorithm was considered and real-time implementation was practiced. Experimental evaluation shows the high precision and low false alarm rate has been achieved for real-world application.

Acknowledgements

This work was supported financially by the Ministry of Economic Affairs under Project No. MOEA 99-EC-17-A-02-S1-032 in Technology Development Program for Academia.

References

[1] P. Gil-Jimenez, R. Lopez-Sastre, P. Siegmann, J. Acevedo-Rodriguez, and S. Maldonado-Bascon, "Automatic Control of Video Surveillance Camera Sabotage," *in Processings of Nature Inspired Problem-Solving Methods in Knowledge Engineering*, Spain, 2007, pp. 222-231.

[2] A. Aksay, A. Temizel, and A. E. Cetin, "Camara tamper detection using wavelet analysis for video surveillance," *IEEE International Conference on Advanced Video and Signal Based Surveillance*, London, 2007, pp. 558-562.

[3] A. Saglam and A. Temizel, "Real-time Adaptive Camera Tamper Detection for Video Surveillance," *IEEE International Conference on Advanced Video and Signal Based Surveillance*, Genova, 2009, pp. 430-435.

[4] E. Ribnick, S. Atev, O. Masoud, N. Papanikolopoulos, and R. Voyles, "Real-Time Detection of Camera Tampering," *IEEE International Conference on Advanced Video and Signal Based Surveillance*, Sydney, 2006, pp. 10-15.

[5] Z. Wang and A.C. Bovik, *Modern Image Quality Assessment*, *San Rafael*, CA: Morgan & Claypool, 2006.

[6] U. Engelke, M. Kusuma, H. J. Zepernick, and M. Caldera, "Reduced-reference metric design for objective perceptual quality assessment in wireless imaging," *Signal Processing: Image Communication,* vol. 24, pp. 525-547, 2009.

[7] P. Shivakumara, B. S. Anami, and G. H. Kumar, "A New Structural No-Reference Rule Based Blur Metric for Classification of Blurred Home Photos," *ECTI Transaction on Electrical Engineering, Electronics and Communications,* vol. 7, no. 1, pp. 73-81, Feb. 2009.

[8] G. Bradski and K. Adrian., *Learning OpenCV,* O'Reilly, September 2008.